Observational Study

Medicine®

OPEN

The impact of dual-source parallel radiofrequency transmission with patient-adaptive shimming on the cardiac magnetic resonance in children at 3.0 T

Haipeng Wang, MD[a], Liyun Qiu, PhD[b], Guangbin Wang, MD, PhD[c], Fei Gao, MD, PhD[c], Haipeng Jia, MD, PhD[d], Junyu Zhao, MD[e], Weibo Chen, MD[f], Cuiyan Wang, MD, PhD[c,*], Bin Zhao, MD, PhD[c,*]

Abstract

The cardiac magnetic resonance (CMR) of children at 3.0 T presents a unique set of technical challenges because of their small cardiac anatomical structures, fast heart rates, and the limited ability to keep motionless and hold breathe, which could cause problems associated with field inhomogeneity and degrade the image quality. The aim of our study was to evaluate the effect of dual-source parallel radiofrequency (RF) transmission on the B1 homogeneity and image quality in children with CMR at 3.0 T. The study was approved by the institutional ethics committee and written informed consent was obtained. A total of 30 free-breathing children and 30 breath-hold children performed CMR examinations with dual-source and single-source RF transmission. The B1 homogeneity, contrast ratio (CR) of cine images, and off-resonance artifacts in cine images between dual-source and single-source RF transmission were assessed in free-breathing and breath-hold groups, respectively. In both free-breathing and breath-hold groups, higher mean percentage of flip angle (free-breathing group: 104.2 ± 4.6 vs 95.5 ± 6.3, $P < .001$; breath-hold group: 101.5 ± 5.1 vs 92.5 ± 6.3, $P < .001$) and lower coefficient of variation (free-breathing group: 0.06 ± 0.02 vs 0.09 ± 0.03, $P < .001$; breath-hold group: 0.07 ± 0.03 vs 0.10 ± 0.04, $P = .005$) were found with dual-source than with single-source RF transmission. Both the CRs in the horizontal long axis (HLA) and short axis of cine images with dual-source RF transmission was improved ($P < .05$ for all). The scores of off-resonance artifacts in the HLA with dual-source RF transmission were higher in both free-breathing and breath-hold groups ($P < .05$ for all), with substantial interreader agreement (kappa values from 0.68 to 0.74). Compared with conventional single-source, dual-source parallel RF transmission could significantly improve the B1 homogeneity and image quality for CMR in children at 3.0 T. This technology could be taken into account in CMR for children with cardiac diseases.

Abbreviations: b-SSFP = balanced steady state free precession, CMR = cardiac magnetic resonance, CR = contrast ratio, CV = coefficient of variation, FA = flip angle, HLA = horizontal long axis, RF = radiofrequency, SA = short axis, TR = repetition time.

Keywords: B1 homogeneity, cardiac magnetic resonance, children, dual-source radiofrequency transmission, image quality

1. Introduction

Cardiac magnetic resonance (CMR) has become a highly reproducible and noninvasive approach for assessing cardiac morphology, function, and myocardial tissue characteristics[1,2] and has been applied widely in a number of cardiac diseases.[3,4] Many CMR diagnostic criteria for cardiac diseases, such as myocarditis,[3] congenital heart disease,[4] and pulmonary hypertension,[5] have been proposed in adults and children. Compared with adults, the CMR of children is significantly different and presents a unique set of technical challenges: the anatomical structures of heart are smaller and the heart rates are faster, which require higher spatial and temporal resolution; the ability to keep motionless and breath-hold in small children is limited,[6,7] which demands free-breathing technologies to decrease or eliminate respiratory bulk motion and through plane motion artifacts. Therefore, CMR scanning protocol in adults might not be suitable for children.

High field (3.0 T) magnetic resonance (MR) could satisfy the high spatial and temporal resolution requirements of children CMR because of its high signal-to-noise ratio (SNR) and contrast-to-noise ratio, especially in certain CMR imaging techniques such as myocardial perfusion imaging,[8] MR spectroscopy,[9] and high-resolution coronary artery imaging.[10] However, 3.0-T MR also causes problems associated with field inhomogeneity, such as standing-wave effects and the pronounced off-resonance artifacts in balanced steady state free

Editor: Heye Zhang.

CW and BZ have contributed equally to the article.

Funding/support: The present study was supported by Provincial Natural Science Foundation of Shandong (ZR2012HM042); Shandong Provincial Natural Science Foundation of China (BS2015YY003); Shandong Provincial Medical and Healthy Technology Development Program of China (2015WS0176).

The authors have no conflicts of interest to disclose.

[a] Department of Radiology, Shandong Provincial Hospital affiliated to Shandong University, [b] Departments of Pharmacy, Jinan Central Hospital, Shandong University, [c] Shandong Medical Imaging Research Institute affiliated to Shandong University, [d] Department of Radiology, Qilu Hospital of Shandong University, [e] Department of Internal Medicine, Shandong Provincial Qianfoshan Hospital, [f] MR Research Collaboration, Philips Healthcare, Shanghai, China.

[*] Correspondence: Bin Zhao, Shandong Medical Imaging Research Institute affiliated to Shandong University, No. 324, Jingqi Road, Huaiyin District, Jinan, Shandong, China (e-mail: zhaobinyys@163.com); Cuiyan Wang, Shandong Medical Imaging Research Institute affiliated to Shandong University, No. 324, Jingqi Road, Huaiyin District, Jinan, Shandong, China (e-mail: cywang0729@163.com).

Medicine (2017) 96:23(e7034)

Received: 2 September 2016 / Received in final form: 7 May 2017 / Accepted: 8 May 2017

http://dx.doi.org/10.1097/MD.0000000000007034

precession (b-SSFP) sequence.[11] Deep sedation with multiple signal averaging in b-SSFP cine imaging was the common method to eliminate the through plane motion artifacts and "average out" the respiratory bulk motion in small children.[12,13] But this approach could more or less decrease the spatial resolution, blur the cardiac structure and lead to the accumulation of radio-frequency (RF) dose, especially at 3.0-T MR.

The application of dual-source parallel RF transmission with patient-adaptive shimming is an approach to improve the B1 homogeneity and cine image quality. With patient-adaptive local RF shimming, the optimal phase and amplitude of 2 independent RF transmission channels could be set and revised automatically for subsequent imaging. Recent studies have shown the advantages of dual-source parallel RF transmission for CMR in adult at 3.0 T,[11,14,15] and MR imaging of the abdomen, pelvis, and spine[16] compared with conventional single-source RF transmission. However, to our knowledge, there is a paucity of studies exploring the application of dual-source RF transmission for CMR in children.

Therefore, the purposes of our study were to evaluate the effect of dual-source parallel RF transmission on the B1 homogeneity and to compare the image quality (contrast ratio [CR] and off-resonance artifacts) of the cine b-SSFP images with and without patient-adaptive local RF shimming in children.

2. Methods and materials

Thirty children with free-breathing scanning (M, 21; median age: 6.5) and 30 children with breath-hold scanning (M, 16; median age: 11.5) were included in the study from Jul 2011 to Dec 2015. They were divided into 2 groups: free-breathing group and breath-hold group. A total of 36 children were clinically diagnosed as suspected myocarditis, 21 as cardiac arrhythmia, 3 children as noncompaction of ventricular myocardium. All children showed normal or mild abnormal cardiac morphology, function, and myocardial tissue characteristics. Exclusion criteria were incomplete CMR examination, contraindications to MR imaging, severe cardiac structure and function abnormality, and severe motion artifact. The study was approved by the institutional ethics committee of Shandong Medical Imaging Research Institute. Written informed consent was obtained from the parents of children.

Children who could cooperate well (usually >7 years) would be instructed how to hold their breaths before the examination, and the MR images were acquired at end-expiratory condition. If they could not hold their breaths (usually <7 years), they would be sedated with 10% chloral hydrate and examined under free-breathing condition.

2.1. CMR imaging protocol

CMR imaging was performed on a clinical whole-body 3.0-T MR imaging system (Achieva 3.0 T TX; Philips Healthcare, Amsterdam, The Netherlands) equipped with flexible dual-source RF transmission technology (dual-source RF, maximal achievable gradient amplitude, 80 mT/m; slew rate, 200/T/m/s). A 16-channel torso phased-array receiver coil was used for signal reception. All data acquisition was retrospective electrocardiograph gated. The images with dual-source RF transmission were acquired when dual-source RF switched on and the images with single-source were acquired when dual-source RF switched off.

For each CMR examination, a cardiac-triggered B1 calibration scan was performed in the horizontal long axis (HLA). The B1 calibration images were acquired utilizing a saturated dual-flip angle (FA) method with a segmented echo-planar imaging read out described by Cunningham et al.[17] The scanning parameters were: repetition time (TR)/echo time, 1000/3.2 milliseconds; nominal FA, 60°; slice thickness, 6 mm; number of slices, 3. The saturation delay of 500 milliseconds was applied to "reset" the magnetization. Based on the B1 calibration images, optimal phase, and amplitude of RF transmit channels with patient-adaptive RF shimming were set and revised automatically for subsequent imaging in the dual-source mode. Although in the conventional quadrature mode, the B1 map without patient-adaptive local RF shimming was also acquired with a fixed phase difference of 90° and identical transmit power of RF transmit channels for intraindividual comparison.

The b-SSFP cine images of all children in the HLA and short axis (SA) were acquired with dual-source RF transmission. The comparative cine images with conventional single-source RF transmission were also acquired at an identical location. The acquisition parameters in free-breathing and breath-hold groups were shown in Table 1.

2.2. Image postprocessing analysis

All the original image data were processed and analyzed with the semiautomated segmentation software on the workstation (EWS; Philips Healthcare).

The B1 maps of 60 children were acquired in the HLA with and without patient-adaptive local RF shimming. The B1 homogeneity was evaluated quantitatively using the achieved mean percentage of nominal FA and its coefficient of variation (CV).[11] High B1 homogeneity performed as high mean percentage and homogeneous distribution of FA, low CV. The parameters of B1 homogeneity were obtained in the B1 maps within a region of interest (ROI) encompassing the entire heart. The ROI was drawn manually on the modulus image and was copied to corresponding B1 map.[15] The mean percentage of FA and standard deviation (SD) within the ROI were calculated automatically and a cumulative histogram that showed the distribution of FA was acquired on the workstation (EWS; Philips Healthcare). The CV of the mean percentage of the FA within the ROI was calculated manually using the formula as follow[11]:[11]:

$$\mathrm{CV} = \text{the mean percentage of}\frac{\mathrm{FA}}{\mathrm{SD}} \quad (1)$$

The CRs with dual-source and single-source RF transmission were evaluated in the HLA and SA of cine images. For each child,

Table 1

The parameters of b-SSFP cine sequence in free-breathing and breathe-hold groups.

	Free-breathing group	Breathe-hold group
TR, ms	Shortest	Shortest
Nominal FA, °	45	45
FOV, mm	280–300	300–320
Image matrix	152 × 166	160 × 179
Slice thickness, mm	6–8	8–10
Number of slices	3	3
Number of heart phases	20	30
NSA	3	1

FA = flip angle, FOV = field of view, NSA = the number of signal averages, TR = repetition time.

A ROI that covered an area of 50 to 100/mm^2 was placed in the interventricular septum (IVS) to measure the mean signal intensity with and without patient-adaptive RF shimming. The mean signal intensity of blood pools of left ventricular (LV) and right ventricle (RV) with and without patient-adaptive RF shimming was also acquired by the same method (avoiding papillary muscle). The CR between IVS and blood pool were calculated as follows[18]:[18]:

$$CR = \frac{SI_{blood\ pool} - SI_{IVS}}{SI_{blood\ pool} + SI_{IVS}} \quad (2)$$

The off-resonance artifacts in the HLA and SA of cine images with dual-source and single-source RF transmission were evaluated independently by 2 experienced CMR radiologists (BZ, 30 years and CYW, 17 years) blinding to clinical data and sequences. Four-point grading scale was used as follow: 4 = no off-resonance artifacts, excellent image quality; 3 = mild off-resonance artifacts, 2 = moderate off-resonance artifacts, and 1 = distinct off-resonance artifacts leading to nondiagnostic image quality.[11]

2.3. Statistical analysis

Categorical data were reported as percentage and continuous data as the mean ± SD. The normality of the variables was assessed by the Shapiro–Wilk test. Student *t* test was performed to compare the mean percentage of FA and CV with and without patient-adaptive RF shimming for B1 homogeneity. To evaluate the image quality between dual-source and single-source RF transmission, CRs was compared using paired *t* test and analysis of variance and off-resonance artifacts were assessed by the Mann–Whitney *U* test. Cohen kappa test was also performed to evaluate the interobserver agreement of off-resonance artifacts, which was defined as follows: a k value of less than 0.2 was indicative of poor agreement, 0.21 to 0.4, fair agreement, 0.41 to 0.6, moderate agreement; 0.61 to 0.80, good agreement; and 0.81 to 1.0, excellent agreement.

All statistical tests were 2-sided, and *P* values less than .05 were considered as statistical significant. The statistical analysis was carried out using SPSS version 19.0 (SPSS INC., Chicago, IL) and MedCalc for Windows, version 12.7.4 (MedCalc Software, Ostend, Belgium).

3. Results

All children in free-breathing and breath-hold groups successfully completed the required CMR examinations, and diagnostic quality data sets were obtained. Clinical characteristics were shown in Table 2.

Table 2

Clinical characteristics in free-breathing and breathe-hold groups.

	Free-breathing group (N = 30)	Breathe-hold group (N = 30)
Demographics		
Male (M, %)	21 (70.0%)	16 (53.3%)
Age, y	6.5 (0.7, 11)	11.5 (7, 18)
Heart rate, bpm	97.8 ± 9.5	82.3 ± 8.8
Clinical diagnosis		
Suspected myocarditis, %	18 (60.0%)	18 (60.0%)
Cardiac arrhythmia, %	11 (36.7%)	10 (33.3%)
NVM, %	1 (3.3%)	2 (6.7%)
Sedated, %	16 (53.3%)	0
LV Cardiac function		
EDV, mL	41.6 ± 1.7	58.8 ± 1.7
ESV, mL	15.6 ± 1.0	20.5 ± 0.7
SV, mL	26.1 ± 0.8	38.3 ± 1.1
LVM, g	26.6 ± 2.3	38.0 ± 2.4
EF, %	63.4 ± 1.5	65.1 ± 0.6

Values are presented as mean ± SD, median (range) or N (%). EDV = end-diastolic volume, EF = ejection fraction, ESV = end-systolic volume, LV = left ventricular, LVM = left ventricular mass, NVM = noncompaction of ventricular myocardium, SV = stroke volume.

3.1. B1 homogeneity

The quantitative analysis for the B1 homogeneity between dual-source and single-source RF transmission is summarized in Table 3. The mean percentage of FA with patient-adaptive dual-source RF transmission was significantly higher than single-source RF transmission in both free-breathing and breath-hold groups (free-breathing group: 104.2 ± 4.6 vs 95.5 ± 6.3, $P < .001$; breath-hold group: 101.5 ± 5.1 vs 92.5 ± 6.3, $P < .001$). For the mean CV of this 2 groups, the dual-source RF transmission was lower than conventional single-source mode (free-breathing group: 0.06 ± 0.02 vs 0.09 ± 0.03, $P < .001$; breath-hold group: 0.07 ± 0.03 vs 0.10 ± 0.04, $P = .005$), indicating a better B1 homogeneity. A representative distribution of the achieved percentage of FA between dual-source and single-source RF transmission is shown in Fig. 1.

3.2. Image quality

In the b-SSFP cine images of free-breathing group, 79 slices in the HLA and 33 slices in the SA were acquired and the CRs with dual-source and single-source RF transmission were evaluated. Both the LV-to-septum and RV-to-septum CRs in the HLA and SA were significantly improved with dual-source RF transmission compared to conventional single-source mode (HLA:CR_{LV}: 0.46 ± 0.075 vs 0.42 ± 0.070, $P < .001$; CR_{RV}:0.54 ± 0.075 vs 0.43 ± 0.081, $P < .001$) (SA:CR_{LV}: 0.49 ± 0.051 vs 0.45 ± 0.060, *P*

Table 3

Comparison of B1 homogeneity between dual-source and single-source radiofrequency transmission in free-breathing and breathe-hold groups.

Groups	B1 homogeneity	Dual-source	Single-source	*P*
Free-breathing group	FA (%)	104.2 ± 4.6	95.5 ± 6.3	<.001*
	CV	0.06 ± 0.02	0.09 ± 0.03	<.001*
Breathe-hold group	FA (%)	101.5 ± 5.1	92.5 ± 6.3	<.001*
	CV	0.07 ± 0.03	0.10 ± 0.04	.005*

Values are presented as mean ± SD. CV = coefficient of variation, FA = mean percentage of flip angle.
* *P* value is significant if <.05.

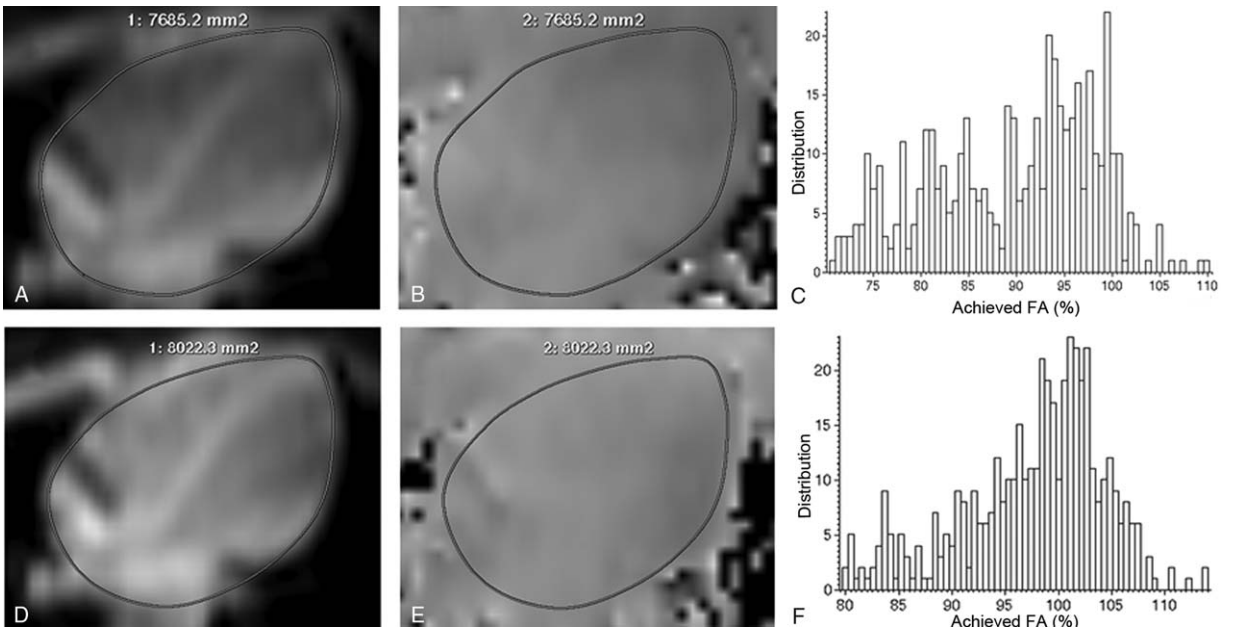

Figure 1. B1 homogeneity data acquisition and image postprocessing. The cardiac modulus images (A and D) and B1 maps (B and E) in the horizontal long axis were acquired with single source (A and B) and dual source (D and E) radiofrequency (RF) transmission. The region of interest was drawn manually on the modulus image (A and D) and copied to corresponding B1 map (B and E). Improved B1 homogeneity was found visually in B1 maps with dual source RF transmission (E) compared with single source RF transmission (B). The distribution of achieved percentage of nominal flip angle (FA) with dual source RF transmission (F) was more concentrated and homogeneous than that with single source RF transmission (C). Besides, the mean percentage of FA was higher with dual source RF transmission (F). FA = flip angle, HLA = horizontal long axis, RF = radiofrequency, ROI = region of interest.

=.023; CR_{RV}: 0.47±0.064 vs 0.35±0.078, $P<.001$). In breath-hold group, 81 slices in the HLA and 47 slices in the SA of cine images were acquired. Similar significant improvement of CRs were also observed (HLA:CR_{LV}: 0.53±0.065 vs 0.46±0.048, $P<.001$; CR_{RV}: 0.58±0.059 vs 0.47±0.066, $P<.001$) (SA: CR_{LV}: 0.54±0.040 vs 0.50±0.041, $P<.001$; 0.48±0.060 vs 0.35±0.072, $P<.001$). The LV (RV)-to-septum CRs in the HLA and SA with dual-source and single-source RF transmission are shown in detail in Fig. 2. A representative signal distribution in line profiles in b-SSFP cine images of free-breathing group with and without patient-adaptive RF shimming is shown in Fig. 3.

In free-breathing group, 16 children (M, 9; median age: 4.5) were sedated. There were no significant statistical differences of LV (RV)-to-septum CRs between sedated children and awake children ($P>.05$ for all). Compared with CRs in breath-hold group, most LV (RV)-to-septum CRs in free-breathing group with dual-source and single-source RF transmission were much lower ($P<.05$, except for RV-to-septum CRs with single-source RF transmission, $P=.109$) (Fig. 4).

The scores of the off-resonance artifacts in the HLA of cine images were significantly higher than that in the SA in both free-breathing and breath-hold groups ($P<.001$ for all). In the HLA of cine images, dual-source RF transmission could significantly reduce the off-resonance artifacts in both free-breathing and breath-hold groups compared with conventional single-source RF transmission (free-breathing group: reader A, 3.39±0.99 vs 2.87±1.34, $P=.028$; reader B, 3.38±1.04 vs 2.84±1.32, $P=.008$) (breath-hold group: reader A, 3.43±1.02 vs 2.84±1.32, $P=.002$; reader B, 3.43±1.01 vs 2.80±1.29, $P=.001$). Interobserver agreement between both 2 readers was good (kappa values from 0.68 to 0.74). However, in SA of cine images with dual-source RF transmission, the off-resonance artifacts could not significantly reduce compared with single-source RF transmission. The scores of off-resonance artifacts are shown in detail in Table 4. The HLA of cine images with off-resonance artifacts with and without RF shimming are shown in Fig. 5.

4. Discussion

In our study, we quantitatively evaluated and compared the effects of dual-source parallel RF transmission with patient-adaptive shimming on the B1 field homogeneity and image quality in children at 3.0-T MR. Compared with conventional single-source, dual-source parallel RF transmission could significantly improve the B1 homogeneity and CRs, reduce the off-resonance artifacts in the HLA of the cine images.

In our study, we found that the dual-source parallel RF transmission could significantly increase the mean percentage of FA, decrease the mean CV and optimize the distribution of FA in both free-breathing and breath-hold groups compared with single-source RF transmission, indicating a more homogenous B1 field. Several approaches, such as postprocessing methods or dielectric cushions,[19] had been used to eliminate or reduce B1 field inhomogeneity at 3.0-T MR, which had a limited effect. Traditional single-source RF transmission provided RF shimming using a fixed anatomy-dependent shimming mode, despite the huge individual anatomical differences in children. Dual-source parallel RF transmission used 2 independent transmission channels, of which the optimal phase and amplitude could be set and revised automatically for subsequent imaging. With this active patient-adaptive RF shimming, the distribution of FA could be optimized and the achieved mean percentage of FA could increase, leading to an improved B1 field homogeneity. As a result, the image homogeneity and myocardial-blood contrast of the images could significantly increase. In our study, we found that the CRs with dual-source RF transmission were significantly improved in free-

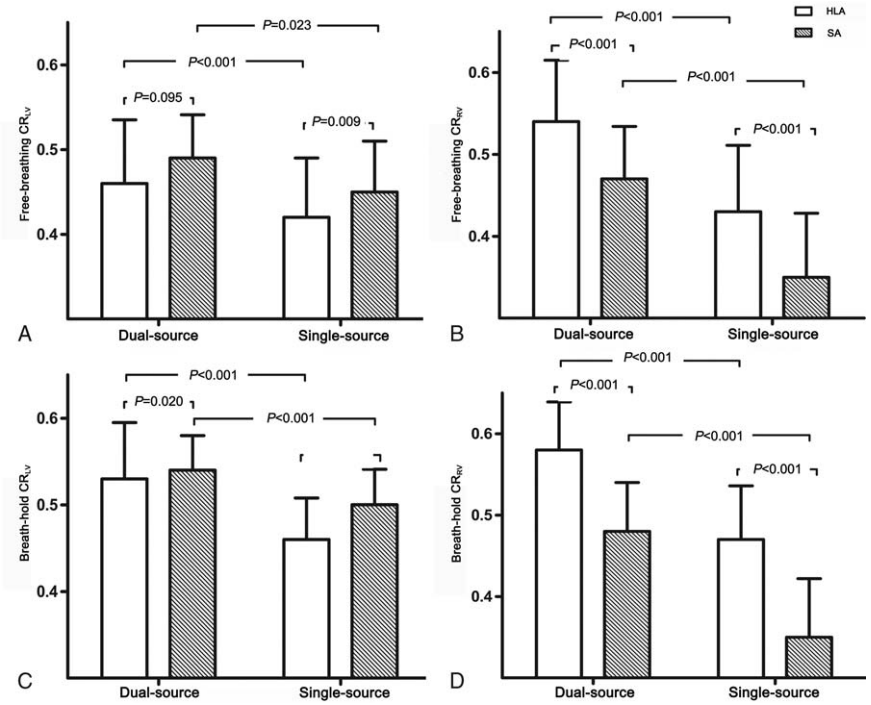

Figure 2. Contrast ratios (CRs) in the horizontal long axis (HLA) and short axis (SA) of cine images in free-breathing and breathe-hold groups. Histogram showed left ventricular-to-septum CRs (A and C) and right ventricular-to-septum CR (B and D) with dual-source and single-source radiofrequency (RF) transmission in both free-breathing (A and B) and breathe-hold (C and D) groups. Compared with single-source RF transmission, dual-source RF transmission could significantly improve the CRs in the HLA and SA of cine images in both free-breathing and breathe-hold groups. CR = contrast ratio, HLA = horizontal long axis, LV = left ventricular, RF = radiofrequency, RV = right ventricular, SA = short axis.

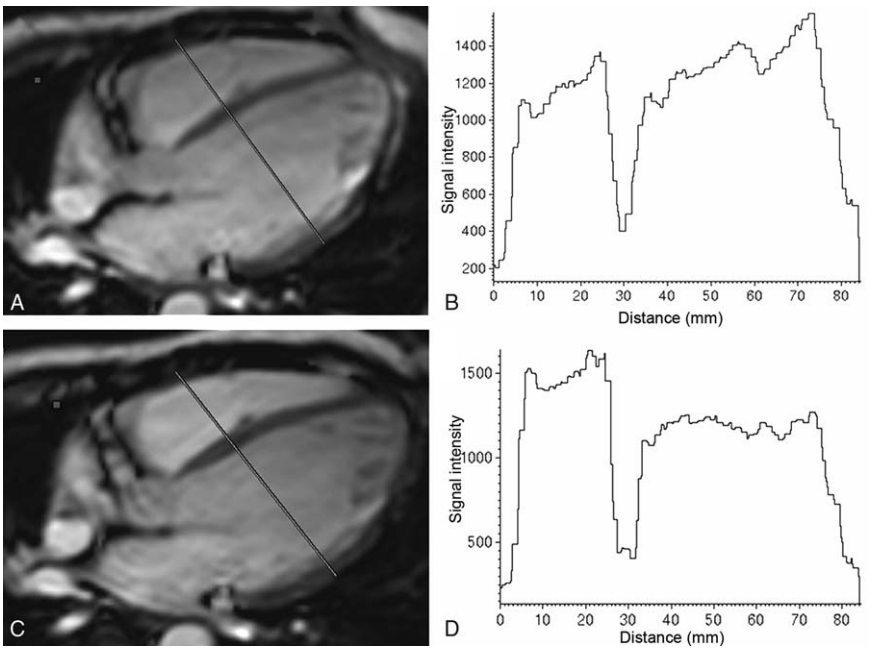

Figure 3. The signal intensity-over-distance curves in the horizontal long axis (HLA) of cine images. Cine images in the HLA (A and C) were obtained with conventional single-source (A and B) and dual-source (C and D) radiofrequency (RF) transmission in free-breathing group. The signal intensity-over-distance curves shown that the signal intensity in both BP and interventricular septum with dual-source RF transmission (D) was more homogeneous than that with single-source RF transmission (B). Besides, the signal contrast at the blood-myocardium border with dual-source RF transmission (D) was more obvious than that with single-source RF transmission (B). BP = blood pool, HLA = horizontal long-axis, IVS = interventricular septum, RF = radiofrequency.

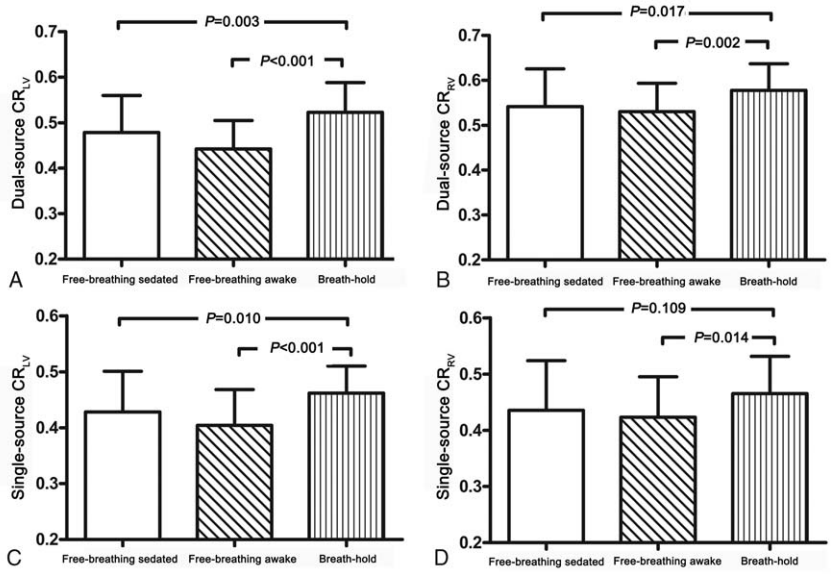

Figure 4. Contrast ratios (CRs) in the horizontal long axis of cine images in sedated and awake children. In free-breathing group, there was no significant statistical difference of left ventricular (LV) (right ventricular [RV])-to-septum CRs between sedated children and awake children. Compared with CRs in breath-hold group, most LV (RV)-to-septum CRs in free-breathing group with dual-source and single-source radiofrequency transmission were much lower. CR = contrast ratio, HLA = the horizontal long axis, LV = left ventricular, RF = radiofrequency, RV = right ventricular.

breathing and breath-hold groups compared with single-source mode. This was consistent with certain studies, which had shown that dual-source parallel RF transmission could improve CRs of CMR in adult[15] and MR imaging of the abdomen, pelvis, and spine at 3.0 T,[16] compared with conventional single-source RF transmission.

In our study, the b-SSFP cine sequence was applied to evaluate the cardiac morphology and function in children at 3.0 T. Cine imaging was one of the cornerstones of CMR examination.[6,20] Nowadays, the b-SSFP cine sequence had become the workhorse of cine imaging at 1.5 T because of its dramatic improvement in SNR and myocardium-blood contrast.[11,21,22] However, the application of b-SSFP sequence at 3.0 T was limited due to significant off-resonance artifacts at the interface of tissues with high susceptibility differences, such as the inferolateral wall of the left ventricle.[23] Combining a higher order shim with a frequency scout was the common method to decrease off-resonance artifacts. The usage of a shorter TR could increase the distance between bands and remove the off-resonance artifacts out of the ROI in CMR.[23,24]

In our study, we found that dual-source RF transmission could significantly reduce the off-resonance artifacts in the HLA of cine images in both free-breathing and breath-hold groups. With the implementation of dual-source RF transmission, the achieved mean percentage of FA was improved and its distribution was more homogeneous. The homogeneity of the B1 field could reduce local specific absorption rate (SAR) peaks and optimize the SAR distribution, which made it possible to lower the TR or increase FA of the SSFP sequences.[11,15,16,25] The minimum TR achievable for cine imaging at 3.0 T could remove the off-resonance artifacts out of the wall of LV.[23] However, in SA of cine images with dual-source RF transmission, the scores of off-resonance artifacts did not significantly higher than that with single-source RF transmission. The off-resonance artifacts in SA always existed in inferolateral walls of LV, which were at the interface of liver, stomach, and myocardium with higher susceptibility differences.[23] The off-

Table 4

Comparison of the scores of off-resonance artifacts between dual source and single source radiofrequency transmission in free-breathing and breathe-hold groups.

Groups		Dual-source	Single-source	*P*	Kappa1	Kappa2
Free-breathing group	$HLA_{(A)}$	3.39 ± 0.99	2.87 ± 1.34	.028*	0.73	0.70
	$HLA_{(B)}$	3.38 ± 1.04	2.84 ± 1.32	.008*		
	$SA_{(A)}$	2.36 ± 1.37	1.67 ± 1.19	.020*	0.64	0.68
	$SA_{(B)}$	2.36 ± 1.37	1.82 ± 1.26	.097		
Breath-hold group	$HLA_{(A)}$	3.43 ± 1.02	2.84 ± 1.32	.002*	0.74	0.68
	$HLA_{(B)}$	3.43 ± 1.01	2.80 ± 1.29	.001*		
	$SA_{(A)}$	2.04 ± 1.30	1.96 ± 1.25	.762	0.75	0.72
	$SA_{(B)}$	2.06 ± 1.33	2.00 ± 1.29	.885		

Values are presented as mean ± SD. Kappa1, kappa values of off-resonance artifacts with dual-source radiofrequency transmission; Kappa2, kappa values of off-resonance artifacts with single source radiofrequency transmission. A = reader A, B = reader B, HLA = horizontal long axis, SA = short axis.

* *P* value is significant if <.05.

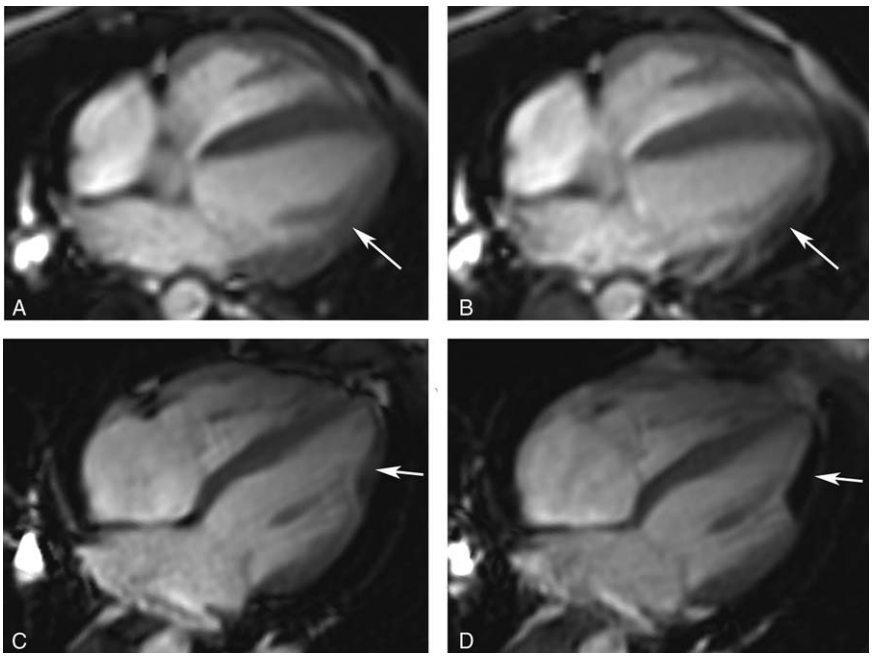

Figure 5. The off-resonance artifacts in the horizontal long axis of cine images with and without patient-adaptive radiofrequency (RF) shimming. The off-resonance artifacts in the cine images were shown in both free-breathing (A and B) and breath-hold (C and D) groups. Compared with single source RF transmission (B and D), the off-resonance artifacts in the cine images with dual-source RF transmission (A and C) were significantly reduced (arrows). HLA = the horizontal long axis, RF = radiofrequency.

resonances artifacts in inferolateral walls of LV were too severe to eliminate with dual-source RF transmission.

In our study, the multiple signal averaging in b-SSFP cine image was applied in small children with free-breathing scanning. It was a common method to "average out" the respiratory motion and the through plane motion artifacts.[12,13] This simple approach increased the number of signal averages (NSAs) to 2 to 3[4] and inherently improved the SNR. But averaging in the presence of significant respiratory motion could more or less decrease the spatial resolution and blur the cardiac structure, especially the endocardial boundary, thereby affecting the assessment of cardiac function.[26] Besides, multiple NSAs led to the accumulation of RF dose and were more inclined to reach the limitation of SAR, especially at 3.0-T MR.

All those disadvantages of multiple NSAs could be resolved by using the dual-source RF transmission. With the significant improvement of blood-to-myocardium contrast in the b-SSFP cine images, the endocardial boundary could be identified more clearly and the cardiac function could be assessed more accurately.[27] In the free-breathing group, we found that the signal contrast at the blood-myocardium border with dual-source RF transmission was more obvious than that with single-source RF transmission (Fig. 3). Besides, improved B1-field homogeneity could reduce local peaks of energy deposition and optimize the distribution of whole body SAR.[11,15]

One of the limitations in our study was that children enrolled in were not healthy children. But all children performed normal or mild abnormal cardiac morphology, function, and myocardial tissue characteristics in CMR. Another limitation was that we only evaluate the effect of dual-source parallel RF transmission on the B1 homogeneity and b-SSFP cine sequences. The values of dual-source parallel RF transmission on the cardiac function, myocardial perfusion imaging, and myocardial tissue characteristics would be discussed in the future.

5. Conclusion

Compared with conventional single-source, dual-source parallel RF transmission with patient-adaptive RF shimming could significantly improve B1 homogeneity and image quality for CMR in children at 3.0 T. This technology could be taken into account in CMR for children with cardiac diseases.

References

[1] Klein C, Nekolla SG, Bengel FM, et al. Assessment of myocardial viability with contrast-enhanced magnetic resonance imaging: comparison with positron emission tomography. Circulation 2002;105:162–7.
[2] Pennell DJ, Sechtem UP, Higgins CB, et al. Clinical indications for cardiovascular magnetic resonance (CMR): consensus panel report. Eur Heart J 2004;25:1940–65.
[3] Raimondi F, Iserin F, Raisky O, et al. Myocardial inflammation on cardiovascular magnetic resonance predicts left ventricular function recovery in children with recent dilated cardiomyopathy. Eur Heart J Cardiovasc Imaging 2015;16:756–62.
[4] Fratz S, Chung T, Greil GF, et al. Guidelines and protocols for cardiovascular magnetic resonance in children and adults with congenital heart disease: SCMR expert consensus group on congenital heart disease. J Cardiovasc Magn Reson 2013;15:51.
[5] Moledina S, Pandya B, Bartsota M, et al. Prognostic significance of cardiac magnetic resonance imaging in children with pulmonary hypertension. Circ Cardiovasc Imaging 2013;6:407–14.
[6] Driessen MM, Breur JM, Budde RP, et al. Advances in cardiac magnetic resonance imaging of congenital heart disease. Pediatr Radiol 2015; 45:5–19.
[7] Buechel ER, Balmer C, Bauersfeld U, et al. Feasibility of perfusion cardiovascular magnetic resonance in paediatric patients. J Cardiovasc Magn Reson 2009;11:51.
[8] Bernhardt P, Gradinger R, Walcher T, et al. Cardiac magnetic resonance adenosine perfusion at 3 Tesla is superior to 1.5 Tesla for detection of relevant coronary artery stenosis. J Cardiovasc Magn Reson 2011;13: 97.
[9] Venkatesh BA, Lima JA, Bluemke DA, et al. MR Proton spectroscopy for myocardial lipid deposition quantification: a quantitative comparison between 1.5-T and 3-T. J Magn Reson Imaging 2012;36:1222–30.

[10] Johnson CP, Weavers PT, Borisch EA, et al. Three-station three-dimensional bolus-chase MR angiography with real-time fluoroscopic tracking. Radiology 2014;272:241–51.
[11] Mueller A, Kouwenhoven M, Naehle CP, et al. Dual-source radio-frequency transmission with patient-adaptive local radiofrequency shimming for 3.0-T cardiac MR imaging: initial experience. Radiology 2012;263:77–85.
[12] Krishnamurthy R, Pednekar A, Atweh LA, et al. Clinical validation of free breathing respiratory triggered retrospectively cardiac gated cine balanced steady-state free precession cardiovascular magnetic resonance in sedated children. J Cardiovasc Magn Reson 2015;17:1.
[13] Abd-Elmoniem KZ, Obele CC, Sibley CT, et al. Free-breathing single navigator gated cine cardiac magnetic resonance at 3 T: feasibility study in patients. J Comput Assist Tomogr 2011;35:382–6.
[14] Krishnamurthy R, Pednekar A, Kouwenhoven M, et al. Evaluation of a subject specific dual-transmit approach for improving B1 field homogeneity in cardiovascular magnetic resonance at 3T. J Cardiovasc Magn Reson 2013;15:68.
[15] Jia H, Wang C, Wang G, et al. Impact of 3.0 T cardiac MR imaging using dual-source parallel radiofrequency transmission with patient-adaptive B1 shimming. PLoS One 2013;8:e66946.
[16] Willinek WA, Gieseke J, Kukuk GM, et al. Dual-source parallel radiofrequency excitation body MR imaging compared with standard MR imaging at 3.0 T: initial clinical experience. Radiology 2010;256: 966–75.
[17] Cunningham CH, Pauly JM, Nayak KS. Saturated double-angle method for rapid B1+ mapping. Magn Reson Med 2006;55:1326–33.
[18] Strach K, Clauberg R, Müller A, et al. Feasibility of high-dose dobutamine stress SSFP cine MRI at 3 Tesla with patient adaptive local RF shimming using dual-source RF transmission: initial results. Rofo 2013;185:34–9.
[19] Franklin KM, Dale BM, Merkle EM. Improvement in B1-inhomogeneity artifacts in the abdomen at 3T MR imaging using a radiofrequency cushion. J Magn Reson Imaging 2008;27:1443–7.
[20] Simonetti OP, Cook S. Technical aspects of pediatric CMR. J Cardiovasc Magn Reson 2006;8:581–93.
[21] Plein S, Bloomer TN, Ridgway JP, et al. Steady-state free precession magnetic resonance imaging of the heart: comparison with segmented k-space gradient echo imaging. J Magn Reson Imaging 2001;14:230–6.
[22] Ruehm J, Goyen SG, Buck M, et al. MR evaluation of ventricular function: true fast imaging with steady-state precession versus fast low-angle shot cine MR imaging: feasibility study. Radiology 2001;219: 264–9.
[23] Rajiah P, Bolen MA. Cardiovascular MR Imaging at 3 T: opportunities, challenges, and solutions. Radiographics 2014;34:1612–35.
[24] Dietrich O, Reiser MF, Schoenberg SO. Artifacts in 3-T MRI: physical background and reduction strategies. Eur J Radiol 2008;65:29–35.
[25] Nelles M, König RS, Gieseke J, et al. Dual source parallel RF transmission for clinical MR imaging of the spine at 3.0 T: intra-individual comparison with conventional single-source transmission. Radiology 2010;257:743–53.
[26] Zhang H, Li B, Young AA, et al. Recovery of myocardial kinematic function without the time history of external loads. EURASIP J Adv Signal Proc 2010;1:7.
[27] Buechel EV, Kaiser T, Jackson C, et al. Normal right- and left ventricular volumes and myocardial mass in children measured by steady state free precession cardiovascular magnetic resonance. J Cardiovasc Magn Reson 2009;11:19.